




**SCIENTIFIC CORRESPONDENCE**

# A rare case of paediatric astroblastoma with concomitant *MN1-GTSE1* and *EWSR1-PATZ1* gene fusions altering management

Karan R. Chadda<sup>1</sup> | Katherine Holland<sup>2</sup> | Daniel Scoffings<sup>3</sup> | Andrew Dean<sup>4</sup> |  
 Jessica C. Pickles<sup>5</sup>  | Sam Behjati<sup>1,6</sup> | Thomas S. Jacques<sup>5,7</sup>  | Jamie Trotman<sup>8</sup> |  
 Patrick Tarpey<sup>8</sup> | Kieren Allinson<sup>4</sup> | Matthew J. Murray<sup>1,9</sup>  |

Genomics England Research Consortium

<sup>1</sup>Department of Paediatric Haematology and Oncology, Cambridge University Hospitals NHS Foundation Trust, Cambridge, UK

<sup>2</sup>Department of Neurosurgery, Cambridge University Hospitals NHS Foundation Trust, Cambridge, UK

<sup>3</sup>Department of Radiology, Cambridge University Hospitals NHS Foundation Trust, Cambridge, UK

<sup>4</sup>Department of Neuropathology, Cambridge University Hospitals NHS Foundation Trust, Cambridge, UK

<sup>5</sup>Developmental Biology and Cancer Department, University College London Great Ormond Street Institute of Child Health, London, UK

<sup>6</sup>Wellcome Trust Sanger Institute, Hinxton, Cambridge, UK

<sup>7</sup>Department of Histopathology, Great Ormond Street Hospital for Children, NHS Foundation Trust, London, UK

<sup>8</sup>100,000 Genomes Project, East of England Genomic Medicine Centre, Cambridge, UK

<sup>9</sup>Department of Pathology, University of Cambridge, Cambridge, UK

**Correspondence**

Matthew J. Murray, Department of Pathology, University of Cambridge, Tennis Court Road, Cambridge, CB2 1QP, UK.

Email: mjm16@cam.ac.uk

**Funding information**

Great Ormond Street Children's Charity; The Brain Tumour Charity; National Institute for Health Research; Olivia Hodson Cancer Fund; CHILDREN with CANCER UK; Cancer Research UK; Wellcome Trust; Medical Research Council

Brain tumours are the commonest childhood neoplasm, with a worldwide incidence of 29.9–47.1/million [1]. Childhood brain tumours carry substantial morbidity/mortality and are the largest cause of paediatric cancer deaths [2]. Historically, classification was largely based on histological features. In recent years, the expansion of high-resolution genomic, epigenetic and transcriptomic profiling has led to improved molecular understanding and categorisation, as well as targeted therapies [3]. Consequently, the 2016 WHO classification incorporated molecular features in some brain tumour entities [4]. According to this classification, astroblastomas are extremely rare, not formally graded, and listed under 'other gliomas'. Astroblastomas are generally treated by surgery alone but can display intermediate behaviour with high recurrence rates and unpredictable behaviour [5,6]. Controversy exists as to whether astroblastomas are a truly distinct entity as they have histological features in common with both astrocytomas and ependymomas [7–9]. Diagnosing astroblastomas is therefore challenging and misclassification can alter subsequent

management [8]. The present case demonstrates how recent molecular advances identified two gene fusions for this patient, confirmed a more precise tumour diagnosis and guided subsequent management decisions. The findings here have general importance to other rare paediatric brain tumour entities.

A 13-year-old girl presented with a 2-week history of morning headaches, vomiting and visual loss. There was no prior history of note. On examination, bilateral papilloedema and central visual field loss were confirmed. MRI head showed a 6.0 × 5.5 × 4.2 cm mixed solid-cystic lesion centred in the right cingulate gyrus/corpus callosum (Figure 1A–C) with associated hydrocephalus, treated with intravenous dexamethasone. No other lesions were identified, and spinal MRI was clear. Serum AFP/HCG tumour markers were negative. The patient underwent a stealth-guided craniotomy with complete macroscopic resection of the frontal tumour. The patient recovered well postoperatively with no complications. Postoperative MRI head scan with contrast showed no residual tumour (Figure 1D).

This is an open access article under the terms of the Creative Commons Attribution License, which permits use, distribution and reproduction in any medium, provided the original work is properly cited.

© 2021 The Authors. *Neuropathology and Applied Neurobiology* published by John Wiley & Sons Ltd on behalf of British Neuropathological Society.

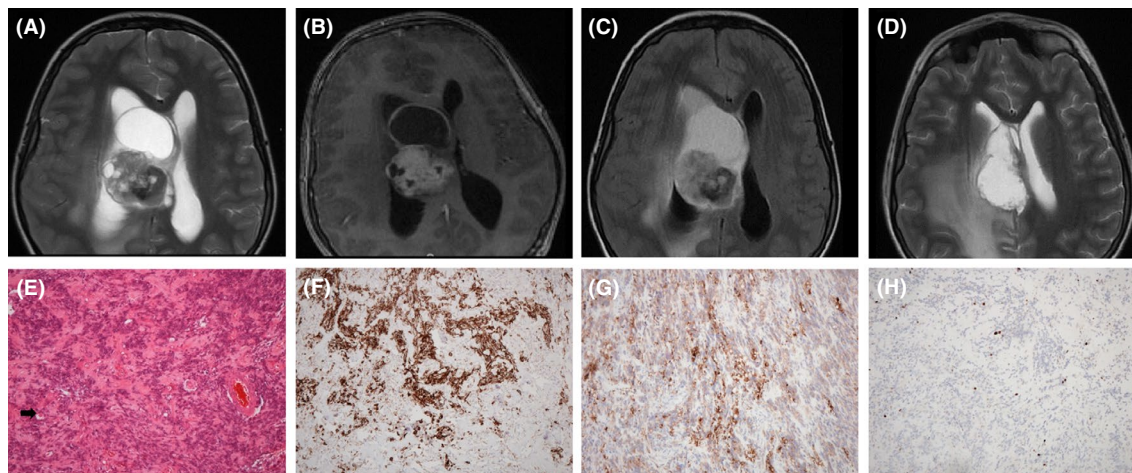


**FIGURE 1** Representative neuroradiological imaging (A–D) and neuropathology (E–H) of the tumour. *Neuroradiology* (A–D): (A) Axial T2W; (B) Axial postgadolinium 3D T1; and (C) Axial FLAIR sequences showed a well-circumscribed solid-cystic tumour in the right cingulate gyrus and corpus callosum, which crossed the midline and extended into the right lateral ventricle. The lesion had a local mass effect causing a large area of surrounding vasogenic oedema and secondary hydrocephalus. The solid components enhanced and contain some areas of low T2W signal intensity from calcification. The large anterior tumoural cyst was of high signal on FLAIR because of proteinaceous content. To assess the vascularity of the tumour preoperatively, digital subtraction angiography was also performed which demonstrated displacement of the anterior cerebral arteries to the left side, consistent with mass effect secondary to tumour, but minimal tumour 'blush' following contrast phasing through the brain centrally. Consequently, no embolisation was performed. (D) Early postoperative axial T2W showing complete resection of the tumour. *Neuropathology* (E–H): all images taken at 10× magnification. (E) Representative haematoxylin and eosin (H&E) staining of the tumour, showing perivascular pseudo-rosette formation (black arrow) and stromal collagenisation; (F) GFAP staining showing strong and diffuse staining in glial cells surrounding blood vessels. Cells with neurocytic differentiation are negative; (G) Synaptophysin staining revealing positivity in cells with neurocytic or neuronal differentiation; (H) Sparse MIB1 staining, confirming a low Ki67 proliferation index (2.5%)

Histological examination demonstrated a cellular neuroepithelial tumour with a perivascular growth pattern forming vague pseudo-rosettes (Figure 1E). In some areas, there was marked stromal and vascular collagenisation. There was no mitotic activity and no microvascular proliferation. The tumour had a generally noninfiltrative border with surrounding brain tissue. There were occasional eosinophilic granular bodies and no Rosenthal fibres or ganglion cell components. The tumour had focal strong staining for GFAP and only weak staining for synaptophysin (Figure 1F/G). There was only very sparse mitotic activity and a low Ki67 proliferation index (2.5%), as evidenced by MIB1 staining (Figure 1H). The histological and immunohistochemical features were most consistent with a diagnosis of astroblastoma.

Methylation profiling of the tumour [10] using the Illumina EPIC array platform and analysed using the DKFZ Heidelberg classifier, gave a very low calibration score of <0.9 (specifically 0.0475 at the time of reporting using classifier version MNPv11b4, and 0.0764 with the most recent version MNPv11b6). These scores were too low for reliable classification despite excellent probe hybridisation (only 0.09% of probes failed), suggesting that the tumour was unclassifiable compared with currently recognised tumour entities. This was confirmed by comparing the tumour's methylation profile with other CNS tumour entities (Figure 2A). Regarding genomic alterations, inter-chromosomal gene fusions involving the *MN1* gene (*MN1-BEND2* and *MN1-CXXC5*) have previously been reported in CNS high-grade neuroepithelial tumours (HGNETs) [11], and recently it has been reported that a proportion of these

CNS-HGNET-*MN1* tumours exhibited histological features compatible with astroblastomas [12]. Following informed consent, whole-genome sequencing (WGS) was performed under the 100,000 Genomes Project [13] and under appropriate ethical approvals. WGS deployed Version 1.8 of the analysis pipeline developed by Genomics England (Supplementary Results). This analysis revealed a quiescent genome harbouring 6,218 substitutions and 1,214 small insertions/deletions. Of these, just 28 genic nonsynonymous variants were identified, all likely benign passengers. In addition, 721 structural variants were reported, almost exclusively concentrated via complex intra- and inter-chromosomal rearrangements between chromosomes 17, 19 and 22. Loss of chromosome 9 was the only additional chromosomal imbalance. Of note, the X chromosome remained intact in this patient, which is often disrupted in CNS-HGNET-*MN1* tumours (Supplementary Results, Figure S1). The structural variant data included a somatically acquired paracentric inversion on the chromosome 22 long arm. The intragenic breakpoints were located in intron 1 of the *MN1* gene and intron 2 of the *GTSE1* gene (Figure 2B). Fluorescent sequencing analysis confirmed the presence of the novel *MN1-GTSE1* gene fusion. The predicted chimeric protein retained the uninterrupted coding sequence of *MN1* exon 1, apposed in frame, with exons 3–12 of *GTSE1*. This pattern of rearrangement closely resembled the genomic features of the previously reported *MN1* gene fusions involving *BEND2* and *CXXC5*. Similar disruptive *MN1* variants were absent from 1,903 other 100,000 Genomes Project cancer cases, mainly derived from breast, ovary, endometrium, colon and

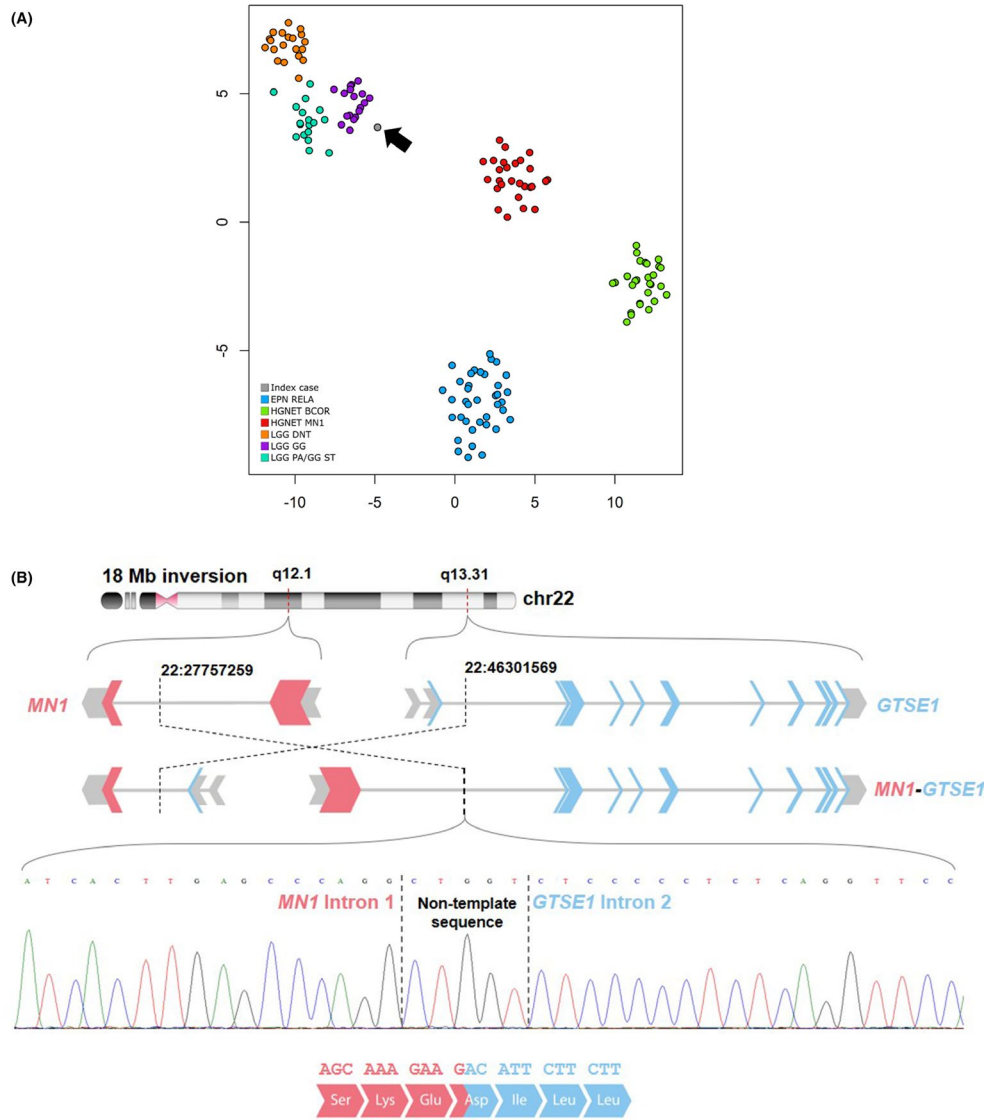


**FIGURE 2** Molecular interrogation of the tumour – *MN1* fusion. (A) t-SNE (t-Distributed Stochastic Neighbour Embedding) plot based on the top 10,000 most variably methylated probes. Parameters used: perplexity = 20, theta = 0.5, dims = 2. The index case was compared with DNA methylation profiles available from DKFZ (Heidelberg Molecular Neuropathology platform, <https://www.molecularneuropathology.org/mnp>) and those held locally [24] with a confirmed molecular classification (calibrated score using MNPv11b6 >0.9). Samples are coloured according to their methylation class: HGNET BCOR: CNS high-grade neuroepithelial tumour with *BCOR* alteration; HGNET MN1: CNS high-grade neuroepithelial tumour with *MN1* alteration; EPN RELA: ependymoma, *RELA* fusion; LG GG: low-grade glioma, ganglioglioma; LG PA/GG ST: low-grade glioma, hemispheric pilocytic astrocytoma and ganglioglioma; LG DNT: low-grade glioma, dysembryoplastic neuroepithelial tumour. The index case is in grey (highlighted by the black arrow), and does not cluster with any of the above entities. (B) Schematic of the genomic rearrangement resulting in a novel *MN1-GTSE1* gene fusion. Whole-genome sequencing detected a somatically acquired 18 megabase (Mb) paracentric inversion on the long arm of chromosome 22, between the cytogenetic bands 22q12.1 and 22q13.31 (top image). The genomic coordinates of the intragenic breakpoints (genome reference build 38) map to intron 1 of the *MN1* gene (NCBI Entrez Gene transcript identifier NM\_016426) and intron 2 of the *GTSE1* gene (transcript NM\_002430) (middle image). This inversion apposes exon 1 of *MN1* to exon 3 of *GTSE1* in the same read direction, causing an *MN1-GTSE1* gene fusion (lower image). Fluorescent sequencing analysis confirmed this fusion, which included nontemplate sequence 'CTGGT'. Upon splicing and transcription, this fusion is predicted to maintain the amino acid read frame and thus result in a novel *MN1-GTSE1* chimeric protein. Key: block arrows represent exons; grey connecting lines represent introns; grey: untranslated regions; red: *MN1* coding exons; blue: *GTSE1* coding exons; Amino acid abbreviations: Ser, serine; Lys, lysine; Glu, glutamic acid; Asp, aspartic acid; Ile, isoleucine; Leu, leucine

kidney. These observations support the functional validity of the novel *MN1-GTSE1* variant reported here. Interestingly, in this tumour, an *EWSR1* (Ewing-Sarcoma-Breakpoint-Region-1) and *PATZ1* (POZ/BTB-And-AT-Hook-Containing-Zinc-Finger-1) (*EWSR-PATZ1*)

gene fusion was also detected. This similarly involved inversion of chromosome 22 and a recent study suggests it may be consistent with a new glioneuronal tumour entity [14]. As a result of this unexpected additional finding, we explored this in more detail. Three

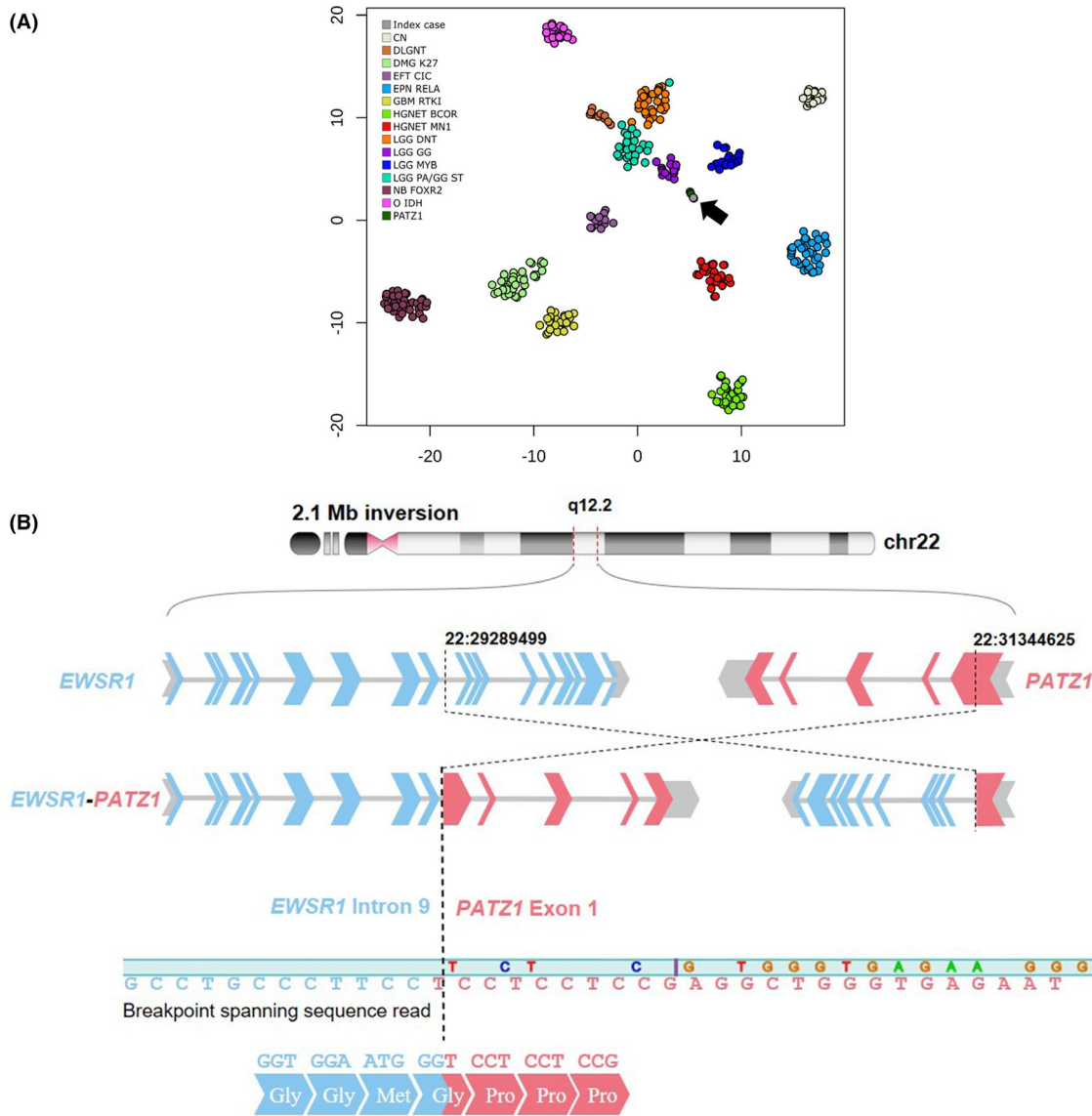


**FIGURE 3** Molecular interrogation of the tumour - PATZ1 fusion. (A) t-SNE plot based on the top 10,000 most variably methylated probes, as in Figure 2A, but with additional cases including three PATZ1-fusion gliomas. Samples are coloured according to their methylation class: CN: central neurocytoma; DLGNT: diffuse leptomeningeal glioneuronal tumour; DMG K27: diffuse midline glioma with H3 K27M mutation; EFT CIC: Ewings-like family tumour with CIC alteration; EPN RELA: ependymoma, RELA fusion; GBM RTKI: glioblastoma receptor tyrosine kinase I group; HGNET BCOR: CNS high-grade neuroepithelial tumour with BCOR alteration; HGNET MN1: CNS high-grade neuroepithelial tumour with MN1 alteration; LGG DNT: low-grade glioma, dysembryoplastic neuroepithelial tumour; LG GG: low-grade glioma, ganglioglioma; LGG MYB: low-grade glioma MYB/MYB1; LG PA/GG ST: low-grade glioma, hemispheric pilocytic astrocytoma and ganglioglioma; NB FOXR2: neuroblastoma FOXR2-altered; O IDH: IDH glioma, 1q/19q codeleted oligodendroglioma; PATZ1: PATZ1-fusion positive cases (identified by TruSight RNA fusion panel, Illumina). The index case is in grey (highlighted by the black arrow), and clusters with the PATZ1 cases (dark green). (B) Schematic of the genomic rearrangement resulting in an EWSR1-PATZ1 gene fusion. Whole-genome sequencing detected a somatically acquired 2.1 megabase (Mb) paracentric inversion on the long arm of chromosome 22, within the cytogenetic band 22q12.2 (top image). The genomic coordinates of the intragenic breakpoints (genome reference build 38) map to intron 9 of the EWSR1 gene (NCBI Entrez Gene transcript identifier NM\_013986) and exon 1 of the PATZ1 gene (transcript NM\_014323) (middle image). This inversion apposes exon 9 of EWSR1 to exon 1 of PATZ1 in the same read direction, causing an EWSR1-PATZ1 gene fusion (lower image). Breakpoint spanning reads in Integrative Genomics Viewer (IGV) evidence this fusion event (paired reads: 28; split reads: 30), mapping to EWSR1 intron 9 and PATZ1 exon 1. This fusion is predicted to maintain the amino acid reading frame and thus result in a EWSR1-PATZ1 chimeric protein. Key: block arrows represent exons; grey connecting lines represent introns; grey: untranslated regions; blue: EWSR1 coding exons; red: PATZ1 coding exons; Amino acid abbreviations: Gly, glycine; Met, methionine; Pro, proline

available glioma cases known to harbour PATZ1 fusions were added to the methylation profiling comparison. Intriguingly, our astroblastoma case, with both MN1 and PATZ1 fusions, remained

distanced from the CNS-HGNET-MN1 tumours but now clustered with the three PATZ1 cases (Figure 3A). Further assessment of the EWSR1-PATZ1 fusion showed that the intragenic breakpoints were

located in intron 9 of the *EWSR1* gene and exon 1 of the *PATZ1* gene (Figure 3B). The position of the rearrangement breakpoints are consistent with those in a reported glioneuronal tumour with an *EWSR1-PATZ1* gene fusion, placing the *PATZ1* breakpoint at the same codon of exon 1, with RNA-sequencing data confirming expression of the chimeric transcript.[14] This report supports the validity of the equivalent *EWSR1-PATZ1* variant reported here. Fusion genes involving *MN1* and *PATZ1* (*MN1-PATZ1*) have also very recently been described in a malignant paediatric brain tumour [15]. We carefully explored our data for evidence of rearrangements (including translocations and tandem duplications) that could similarly adjoin *MN1* and *PATZ1* in functional orientation. We did not find evidence supporting this proposition. However, amidst the rearrangement complexity, we cannot exclude the presence of undetected cryptic events, as have been observed to generate oncogenic fusions in human cancer [16].

Astroblastomas are associated with high recurrence rates and an unpredictable biological course [5,6], with initial peri-tumoural oedema, as was present in this case, associated with early recurrence [17]. Consequently, with the molecular confirmation of an astroblastoma, the multi-disciplinary-team outcome was to undertake MRI surveillance at 3-monthly intervals for the first year of follow-up, instead of the more conservative 6-monthly scan schedule generally associated with low-grade tumours. At subsequent review, the bilateral papilloedema had resolved and there were no abnormal neurological findings on examination. All subsequent MRI scans have showed no tumour recurrence over a 36-month postoperative period, with the frequency of scans being reduced over time (3-monthly first year; 4-monthly second year; 6-monthly in the third year).

Here, we describe a patient with a rare astroblastoma, where additional molecular study assisted patient management. Neuropathologically, the differential diagnoses were an astroblastoma or glioneuronal tumour. Precise diagnosis is critical as it influences postoperative management decisions. Here, the molecular confirmation of the novel *MN1-GTSE1* gene fusion, diagnostic of astroblastoma, supported the team in recommending 3-monthly follow-up, rather than the standard 6-monthly approach which would be more typical for a glioneuronal tumour.

Astroblastomas typically arise at supratentorial sites, although occasional infratentorial cases occur [18,19]. On MRI, they appear as well-demarcated solid-cystic lesions and typically extend from cortex to periventricular regions [20]. Commonly, calcification is seen in addition to a 'bubbly' appearance, arising from signal voids due to tumour angioarchitecture [21,22]. The lesions are typically hyperintense to white matter (FLAIR/T2-weighted sequences) and show heterogeneous enhancement with rim enhancement on contrast-enhanced CT and T1-weighted MRI [9,22]. Our case showed many of these neuroradiological features (Figure 1A-C).

Histologically, astroblastomas are characterised by perivascular hyalinisation and pseudo-rosettes [8]. While these pseudo-rosettes contribute to the diagnostic criteria, they may be completely undetectable [12]. A lack of fibrillary background, hyalinised vessels, and a compressive, rather than infiltrative,

margin is also commonly observed [20]. Immunohistochemically, astroblastomas are typically positive for GFAP, vimentin and S-100 protein [20], although there is variability in staining [8]. Although there is currently no formal grading for astroblastomas (based on the 2016 WHO classification), a putative informal system has been suggested, with 'high-grade' tumours showing high cellularity, anaplastic nuclear features, vascular proliferation, high mitotic rates and necrosis [12], which may be considered for inclusion in future classifications.

Molecular data for astroblastomas are limited [23]. This is consistent with methylation profiling being uninformative in this case, despite its overall utility for paediatric brain tumours [24]. Interestingly, despite re-running the classifier again in 2020, the calibration score of 0.0764 was again too low for reliable classification. DNA methylation studies on CNS high-grade neuroepithelial tumours (CNS-HGNETs) revealed a distinct methylation cluster of recurrent meningioma-1 (*MN1*) gene rearrangements on chromosome 22q. The majority of astroblastomas matched the CNS-HGNET-*MN1* tumour cluster (not seen here; Figure 2A) and approximately 40% of the CNS-HGNETs with *MN1* alteration showed histological features of astroblastomas. Furthermore, RNA sequencing revealed two inter-chromosomal gene fusions involving the *MN1* gene (*MN1-BEND2* and *MN1-CXXC5*) [11,12]. Thus, it is plausible that the genetic basis of astroblastomas may involve *MN1* rearrangement with fusion partner genes, such as *BEND2*, *CXXC5* and other unidentified genes [12]. This is supported by another study showing *MN1* alterations in four of eight tumours diagnosed histologically as astroblastomas [25]. In our patient, we confirmed a novel *MN1-GTSE1* gene fusion, which to our knowledge, is the first such description in an astroblastoma. Interestingly, we also observed an *EWSR1-PATZ1* fusion generated through the rearrangement complexity emanating on chromosome 22, which has been described in glioneuronal tumours and sarcoma [14,26]. Whilst it is unusual to find two oncogenic gene fusions in the same tumour, this is not unprecedented [27]. It may represent the development of two parallel clones with uniform (i.e. nonbiphasic) histology or a double hit within the same clone.

From a diagnostic perspective, our observation of two fusions in this case are intriguing, as without WGS neither fusion would have been detected and our retrospective, integrated interpretation, requiring up-to-date molecular subtyping for context, was critical, despite the astroblastoma histology. We believe that this case is unlikely to represent a typical CNS-HGNET-*MN1* tumour, due to the dissimilarity in methylation profile compared with reference HGNET-*MN1* cohorts, the similarity with *PATZ1*-fusion cases and the intact X chromosome seen here (frequently disrupted in HGNET-*MN1* tumours). Such questions will be answered more definitively in time, as our diagnostic services move away from single-gene testing to WGS and other NGS sequencing technologies, alongside methylation profiling, for CNS tumours. Single-gene testing for *MN1* (e.g. break-apart FISH or PCR) is not available via our standard clinical practices, despite *MN1* FISH data being described in the literature. However, in England, all children with CNS tumours are now eligible

for commissioned WGS via Genomics England. We would therefore expect to identify gene fusions and their variants via this route.

In conclusion, astroblastomas are rare brain tumours with an unpredictable biological course and recurrence pattern, that present potential diagnostic challenges. Despite noninformative methylation studies, this case highlighted a novel *MN1-GTSE1* gene fusion detected on WGS, in keeping with other studies of *MN1* gene alterations in astroblastomas and supported increased frequency of standard MRI surveillance. The additional detection of a second *EWSR1-PATZ1* fusion highlights the complexity of such cases. Recent expansion of high-resolution genomic and other molecular profiling for paediatric brain tumours is likely to continue to lead to improved diagnostic and prognostic techniques, with consequent positive impacts on patient management.

### ACKNOWLEDGEMENTS

This research was made possible through access to the data and findings generated by the 100,000 Genomes Project. The 100,000 Genomes Project is managed by Genomics England Limited (a wholly owned company of the Department of Health and Social Care). The 100,000 Genomes Project is funded by the National Institute for Health Research and NHS England. The Wellcome Trust, Cancer Research UK and the Medical Research Council have also funded research infrastructure. The 100,000 Genomes Project uses data provided by patients and collected by the National Health Service as part of their care and support. TSJ is grateful for funding from Great Ormond Street Children's Charity, The Brain Tumour Charity, Children with Cancer UK, Cancer Research UK, NIHR and the Olivia Hodson Cancer Fund. All research at GOSH NHS Foundation Trust and UCL Great Ormond Street Institute of Child Health is made possible by the NIHR GOSH Biomedical Research Centre. The views expressed are those of the authors and not necessarily those of the NHS, the NIHR or the Department of Health.

### CONFLICTS OF INTEREST

TSJ is Editor-in-Chief of the journal. All other authors have no conflicts to declare. The Editors of Neuropathology and Applied Neurobiology are committed to peer-review integrity and upholding the highest standards of review. As such, this article was peer-reviewed by independent, anonymous expert referees and the authors (including TSJ) had no role in either the editorial decision or the handling of the paper.

### AUTHOR CONTRIBUTION

Study concept: KA, MJM; Methodology: KC, JCP, SB, TSJ, KA, MJM; Data analysis and interpretation: KC, JCP, SB, TSJ, JT, PT, KA, MJM; Literature Review: KC, KA, MJM; Figure acquisition/production: DS, JCP, TSJ, JT, PT, KA, MJM; Clinical input: KH, DS, AD, KA, MJM; Manuscript writing: KC, KA, MJM; Manuscript revision and approval: KC, KH, DS, AD, JCP, SB, TSJ, JT, PT, KA, MJM.

### DATA AVAILABILITY STATEMENT

Data available upon reasonable request.

### ORCID

Jessica C. Pickles  <https://orcid.org/0000-0001-7888-1723>

Thomas S. Jacques  <https://orcid.org/0000-0002-7833-2158>

Matthew J. Murray  <https://orcid.org/0000-0002-4480-1147>

### REFERENCES

1. Abubakar DS, Traunecker HC. Current perspectives on childhood brain tumours: a review. *Paediatrics and Child Health*. 2014;24(4):155-160.
2. Dang M, Phillips PC. Pediatric Brain Tumors. *Continuum*. 2017;23(6, Neuro-oncology):1727-1757.
3. Pollack IF, Agnihotri S, Broniscer A. Childhood brain tumors: current management, biological insights, and future directions. *J Neurosurg Pediatr*. 2019;23(3):261-273.
4. Louis DN, Perry A, Reifenberger G, et al. The 2016 World Health Organization Classification of Tumors of the Central Nervous System: a summary. *Acta Neuropathol*. 2016;131(6):803-820.
5. Bhalerao S, Nagarkar R, Adhav A. A case report of high-grade astroblastoma in a young adult. *CNS. Oncol*. 2019;8(1):CNS29.
6. Samples DC, Henry J, Yu FF, Bazan C, Tarasiewicz I. A case of astroblastoma: Radiological and histopathological characteristics and a review of current treatment options. *Surg Neurol Int*. 2016;7(Suppl 40):S1008-S1012.
7. Port JD, Brat DJ, Burger PC, Pomper MG. Astroblastoma: radiologic-pathologic correlation and distinction from ependymoma. *AJNR Am J Neuroradiol*. 2002;23(2):243-247.
8. Hammas N, Senhaji N, Alaoui Lamrani MY, et al. Astroblastoma - a rare and challenging tumor: a case report and review of the literature. *J Med Case Rep*. 2018;12(1):102.
9. Eom KS, Kim JM, Kim TY. A Cerebral Astroblastoma Mimicking an Extra-axial Neoplasm. *J Korean Neurosurg Soc*. 2008;43(4):205-208.
10. Perez E, Capper D. Invited Review: DNA methylation-based classification of paediatric brain tumours. *Neuropathol Appl Neurobiol*. 2020;46(1):28-47.
11. Sturm D, Orr BA, Toprak UH, et al. New Brain Tumor Entities Emerge from Molecular Classification of CNS-PNETs. *Cell*. 2016;164(5):1060-1072.
12. Hirose T, Nobusawa S, Sugiyama K, et al. Astroblastoma: a distinct tumor entity characterized by alterations of the X chromosome and *MN1* rearrangement. *Brain Pathol*. 2018;28(5):684-694.
13. Caulfield M, Fowler T, Billins T, et al. The National Genomics Research and Healthcare Knowledgebase. Amendment to the 100,000 Genomes Project Protocol v4. May 2019. <https://www.genomicsengland.co.uk/>. Accessed 5th December 2020.
14. Siegfried A, Rousseau A, Maurage CA, et al. *EWSR1-PATZ1* gene fusion may define a new glioneuronal tumor entity. *Brain Pathol*. 2019;29(1):53-62.
15. Burel-Vandenbos F, Pierron G, Thomas C, et al. A polyphenotypic malignant paediatric brain tumour presenting a *MN1-PATZ1* fusion, no epigenetic similarities with CNS High-Grade Neuroepithelial Tumour with *MN1* Alteration (CNS HGNET-MN1) and related to *PATZ1*-fused sarcomas. *Neuropathol Appl Neurobiol*. 2020;46(5):506-509.
16. Anderson ND, de Borja R, Young MD, et al. Rearrangement bursts generate canonical gene fusions in bone and soft tissue tumors. *Science*. 2018;361(6405):eaam8419. <https://doi.org/10.1126/science.aam8419>.
17. Janz C, Buhl R. Astroblastoma: report of two cases with unexpected clinical behavior and review of the literature. *Clin Neurol Neurosurg*. 2014;125:114-124.
18. Denaro L, Gardiman M, Calderone M, et al. Intraventricular astroblastoma. Case report. *J Neurosurg Pediatr*. 2008;1(2):152-155.
19. Ahmed KA, Allen PK, Mahajan A, Brown PD, Ghia AJ. Astroblastomas: a Surveillance, Epidemiology, and End Results (SEER)-based patterns of care analysis. *World Neurosurg*. 2014;82(1-2):e291-e297.

20. Singh DK, Singh N, Singh R, Husain N. Cerebral astroblastoma: A radiopathological diagnosis. *J Pediatr Neurosci*. 2014;9(1):45-47.
21. Navarro R, Reitman AJ, de Leon GA, Goldman S, Marymont M, Tomita T. Astroblastoma in childhood: pathological and clinical analysis. *Childs Nerv Syst*. 2005;21(3):211-220.
22. Bell JW, Osborn AG, Salzman KL, Blaser SI, Jones BV, Chin SS. Neuroradiologic characteristics of astroblastoma. *Neuroradiology*. 2007;49(3):203-209.
23. Mellai M, Piazzini A, Casalone C, et al. Astroblastoma: beside being a tumor entity, an occasional phenotype of astrocytic gliomas? *Oncol Targets Ther*. 2015;8:451-460.
24. Pickles JC, Fairchild AR, Stone TJ, et al. DNA methylation-based profiling for paediatric CNS tumour diagnosis and treatment: a population-based study. *Lancet Child Adolesc Health*. 2020;4(2):121-130.
25. Wood MD, Tihan T, Perry A, et al. Multimodal molecular analysis of astroblastoma enables reclassification of most cases into more specific molecular entities. *Brain Pathol*. 2018;28(2):192-202.
26. Watson S, Perrin V, Guillemot D, et al. Transcriptomic definition of molecular subgroups of small round cell sarcomas. *J Pathol*. 2018;245(1):29-40.
27. Wegert J, Vokuhl C, Collord G, et al. Recurrent intragenic rearrangements of EGFR and BRAF in soft tissue tumors of infants. *Nat Commun*. 2018;9(1):2378.

#### SUPPORTING INFORMATION

Additional supporting information may be found online in the Supporting Information section.

**How to cite this article:** Chadda KR, Holland K, Scoffings D, et al. A rare case of paediatric astroblastoma with concomitant MN1-GTSE1 and EWSR1-PATZ1 gene fusions altering management. *Neuropathol Appl Neurobiol*. 2021;00:1–7. <https://doi.org/10.1111/nan.12701>